Supplementary Information for

Active-modulated, random-illumination, super-resolution optical fluctuation imaging

Baoju Wang[1]*, Zhijia Liu[1]*, Li Zhou[2], Yiyan Fei[1], Chengliang Yang[3], Lan Mi[1**], Quanquan Mu[3**] and Jiong Ma[1,4,5**]

[1]Department of Optical Science and Engineering, Shanghai Engineering Research Center of Ultra-precision Optical Manufacturing, Key Laboratory of Micro and Nano Photonic Structures (Ministry of Education), Green Photoelectron Platform, Fudan University, 220 Handan Road, Shanghai 200433, China

[2]School of Life Sciences, Fudan University, Shanghai 200438, China

[3]State Key Laboratory of Applied Optics, Changchun Institute of Optics, Fine Mechanics and Physics, Chinese Academy of Sciences, Changchun, 130033, China

[4]Insititute of Biomedical Engineering and Technology, Academy for Engineer and Technology, Fudan University, 220 Handan Road, Shanghai 200433, China

[5]The Multiscale Research Institute of Complex Systems (MRICS), School of Life Sciences, Fudan University, 220 Handan Road, Shanghai 200433, China

*These authors contributed equally to this work.

Correspondence: L Mi. Email: lanmi@fudan.edu.cn

Q Mu. Email: muquanquan@ciomp.ac.cn

J Ma. Email: jiongma@fudan.edu.cn

Methods

The simulation flow about the method of active-modulated random illumination to achieve AR-SOFI reconstruction.

The simulation flow about the method of active-modulated random illumination was provided to achieve AR-SOFI reconstruction as shown in the Supplementary Figure S1. In simulation, the image sequences were generated at first. Each image in sequences was regarded as a matrix. Each element of the matrices was independent by the time and the ratio of its value could be modulated. The former step was equivalent to the modulated process of SLM by the control of imported patterned image sequences. After excited laser being modulated by the SLM, it would be into the objective. And then, it would be affected by the diffraction limit. In the simulation, we used a convolution algorithm which convoluted the images with PSF matrices. Then, the modulation of the light field could be represented by these image sequences. Subsequently, the modulated excited laser reached the sample plane and excited the fluorescence markers. In simulation, the light field and sample matrix were multiplied. The elements other than fluorescence dots were zero in the matrices and could not emit fluorescence. In this step, spontaneous fluorescent blinking of fluorescent markers was added. In optical system, the fluorescence was again affected by the diffraction limit when it was collected through the objective. So, the convolution algorithm was used again. Finally, the b-SOFI algorithm was executed to the result sequences and the final different order SOFI reconstructions were obtained [1].

The relevant simulations of active-modulated random illumination to achieve AR-SOFI reconstruction under different conditions

The relevant simulations of active-modulated random illumination to achieve AR-SOFI reconstruction were provided under different conditions, such as different intrinsic blinking on-time ratio (95% or 80%), as shown in the Supplementary Figure S2-S3. For the Supplementary Figure S2 and S3, according to the theoretical formula of the diffraction limit ($0.61\lambda / NA$，λ=$488nm, NA = 1.45$), the PSF's FWHM of every random excited illumination region was 205 nm and the PSF's FWHM of emission was about 250 nm. In the simulation, the distance between adjacent two points was 106 nm and the two points were imaging by convolution PSF (250 nm). Due to the diffraction limit, the two points could not be resolved, as shown in the Supplementary Figure S2(a, c and i). when the fluorescence of two points is non-modulation and non-blinking, the cumulants are zero in 2nd, 3rd, and 4th order SOFI reconstruction, as shown in the Supplementary Figure S2(b)-(d). Suppose the fluorescence of two points existed intrinsic blinking and the blinking on-time ratio was about 95%, 1000-frame original images were used to reconstruct 2nd, 3rd, and 4th order SOFI, as shown in Supplementary Figure S2(f)-(h). Although the sizes of PSFs were decreased, the two points were still not resolved. We think the impertinent blinking on-time ratio lead artifacts which affected the power of resolution, as depicted in the Supplementary Figure S2(h). In addition, the previous researches also reported that impertinent blinking on-time ratio affected the power of resolution [2, 3]. Compared with different order SOFI reconstruction relying on intrinsic blinking of fluorescent markers, the combination of active-modulated random illumination and intrinsic blinking of fluorescent markers shown the advantages for different order SOFI reconstruction by controllable blinking on-time ratio, as shown in the Supplementary Figure S2(j)-(l). In addition, compared with conventional 4th order SOFI, the two points were well distinguished in 4th order AR-SOFI, as shown in the Supplementary Figure S2(h) and S2(l). The resolving power of the 4th order AR-SOFI was approximately 109 nm, which was basically the same as the data of Figure 4(q) in original manuscript. Similarly, the original manuscript shown the blinking on-time ratio of quantum dots (QDs) was distributed at 80%. Therefore, the combined effects of active-modulated random illumination and intrinsic blinking on-time ratio 80% of fluorescent markers were also simulated and shown in the Supplementary Figure S3.

Optical experiment setup

A lab-made optical system was built to perform active-modulated random illumination and imaging, as shown in Figure 2(b). The 488 nm laser beam was generated by a continuous wavelength, single-mode diode laser. Two pairs of beam expanders were placed in the optical path to expand the beam. The polarization beam splitter and half-wave plate were used to control the polarization direction of the beam. The spatial light modulator (SLM, LETO HOLOEYE Photonics AG) was used to generate random lattice illumination with on-time information based on a series of modulation patterns. The size of the entire modulated region was 6.912 *mm*×6.912 *mm* and the entire modulated region was made up of 216×216 arrays. Additionally, the size of every modulated region on the SLM was 32 μm. The relationship of position of the SLM and the imaging plane of the objective was conjugated. Subsequently, a polarization beam splitter was used to ensure the polarization direction. The laser beam was then reflected by a 495nm long-pass dichroic mirror. Meanwhile, a long-focus 500 mm lens (L5) was placed between the SLM and an oil-immersed objective (150×/1.45, Olympus). The distance between lens (L5) and SLM was 500 mm. At the same time, the magnification factor of the combination of the objective and lens (L5) was approximately 420×. Therefore, the small light or dark

regions were approximately 76 nm on the imaging plane of objective. For the achievement of modulated on-time ratio illumination, every small modulated illumination region was set in advance based on a series of modulation patterns. When the 1000-frame fluorescent images (exposure time: 20ms/frame) were captured, the modulated patterns of 1000 frames were continuously input into the SLM at the rate of 20 ms/frame. Therefore, the on-time ratio information of the modulated illumination could be attached a series of fluorescent images. It meant that the final distribution of on-time ratio was the superposition of the intrinsic on-time ratio of fluorescent markers and on-time ratio of modulated illumination. Therefore, after measuring the intrinsic on-time ratio of fluorescent markers, the specific on-time ratio of modulated illumination was set to obtain the proper final distribution of on-time ratio corresponding to the optimal cumulants of different order SOFI processing. The emission was collected through the same objective and filtered by a 520 nm band-pass filter (FF01-520/35-25, Semrock) for Alexa 488 or by a 655 nm band-pass filter (FF02-655/40-25, Semrock) for QDs655 and was then captured by an electron multiplying charge coupled device (EMCCD, Evolve 512 Delta Photometrics)

Image acquisition and processing

1000-frame wide-field images were recorded by using an oil-immersed objective (150×/1.45, Olympus) and EMCCD (Evolve 512 Delta Photometrics). The exposure time was 20 ms. The pixel size is approximately 106.7nm. For SOFI reconstruction, the statistical analyses of cumulants were based on the raw spatiotemporal cross-cumulant and the -th root linearization algorithm [1]. In this study, 1000-frame original images were used for different order SOFI reconstruction with the shortest accessible lag time. For continuous analysis, Skeletonize 3D (download from http://imagej.net/Skeletonize3D), a plugin developed by Fiji, was employed to obtain the skeleton of the microtubules and represented the geometrical and topological features of the original structure [4]. At the same time, AnalyzeSkeleton (2D/3D) (download from https://imagej.net/AnalyzeSkeleton) a plugin developed by Fiji, was used to analyze the length of skeleton of the microtubules [5].

Cell culture and immunofluorescence staining

BSC-1 cells were obtained from BeNa Collection China and cultured in Modified Eagle Medium basic (Gibco) supplemented with 10% fetal bovine serum (Gibco), 100 U/ml penicillin, 100 μg/ml streptomycin and Nonessential Amino Acid (Gibco). The cells were plated onto glass bottom dishes coated with 10μg/ml fibronectin (EMD Millipore) and allowed to grow for 16 hours in 37 ℃.

For microtubule staining, cells were pretreated with extracting buffer (0.1 M PIPES, 1 mM EGTA, 1mMMgcl2, 0.2% v/v Triton X-100) for 40s and washed with PBS, and fixed with 4% paraformaldehyde and 0.1% v/v glutaraldehyde in PBS for 15 min. After fixation, cells were permeabilized with 0.5% v/v Triton X-100 for 5 min and blocked with 1% bovine serum albumin, 5% donkey serum and 0.5% v/v Triton X-100 for 30 min. The cells were stained in anti-alpha tubulin antibodies (Abcam, ab18251) with a dilution of 1:200 for 1hr, and washed 3 times with PBS. Cells were then stained for 2hr with Alexa 488 (Abcam, ab150077) or QDs655 (Thermo Fisher Scientific, Q11422MP) in blocking buffer and washed in PBS three times. All the staining treatment was carried out at room temperature.

Supplementary Figures

The simulation flow about this method; The relevant simulations of this method under different conditions; A comparison of photostability of Alexa488 with modulation and non-modulation; A comparison between 5th–7th order SOFI and 5th–7th order AR-SOFI and resolution enhancement of different order of AR-SOFI images of microtubules of BS-C-1 cells labelled with Alexa 488 or QDs655; A compared assessment of image qualities between traditional SOFI and AR-SOFI; The statistical distribution of the on-time ratio based on single-particle statistics for quantum dot; A comparison between SOFI and AR-SOFI using 8000-frame wide-field images, A comparison of between 4th order AR-SOFI and SOFI under controllable different on-time ratio, A comparison of the continuities of 4th order SOFI and 4th order AR-SOFI;

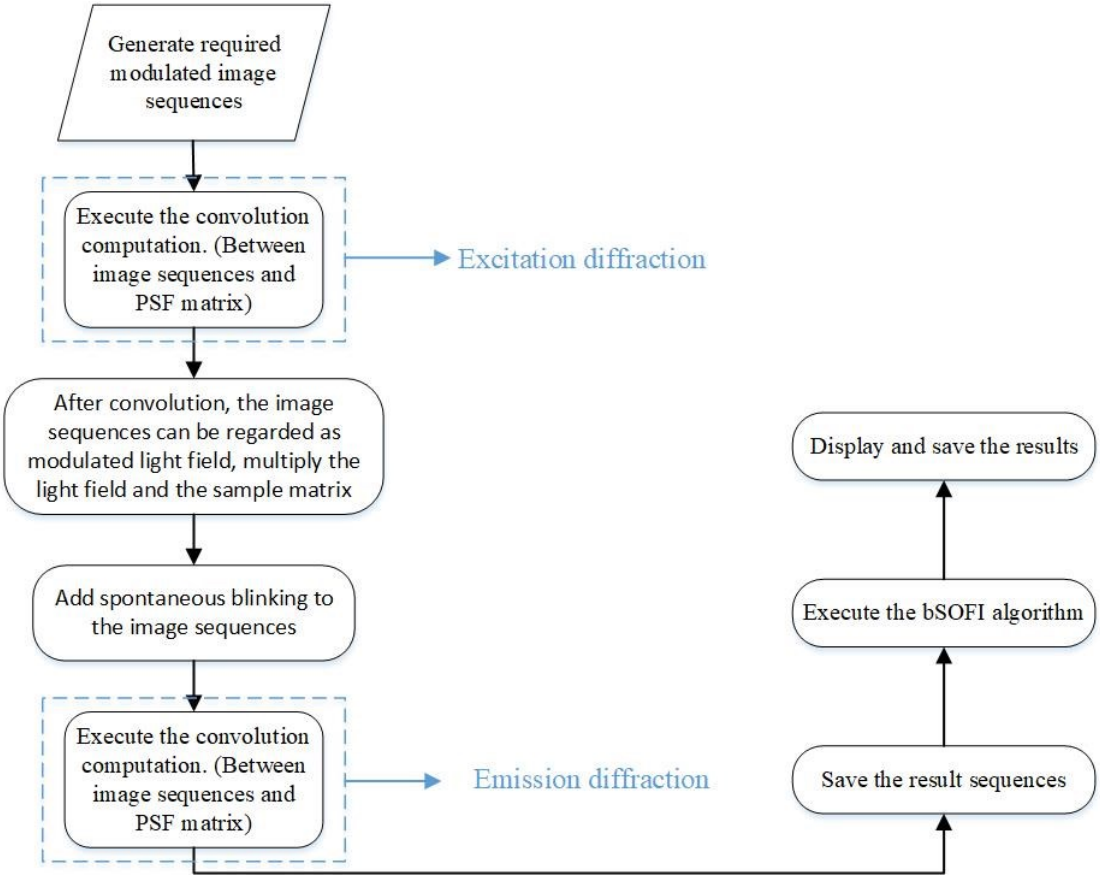

Supplementary Figure S1 The simulation flow about the method of active-modulated random illumination to achieve high order SOFI reconstruction.

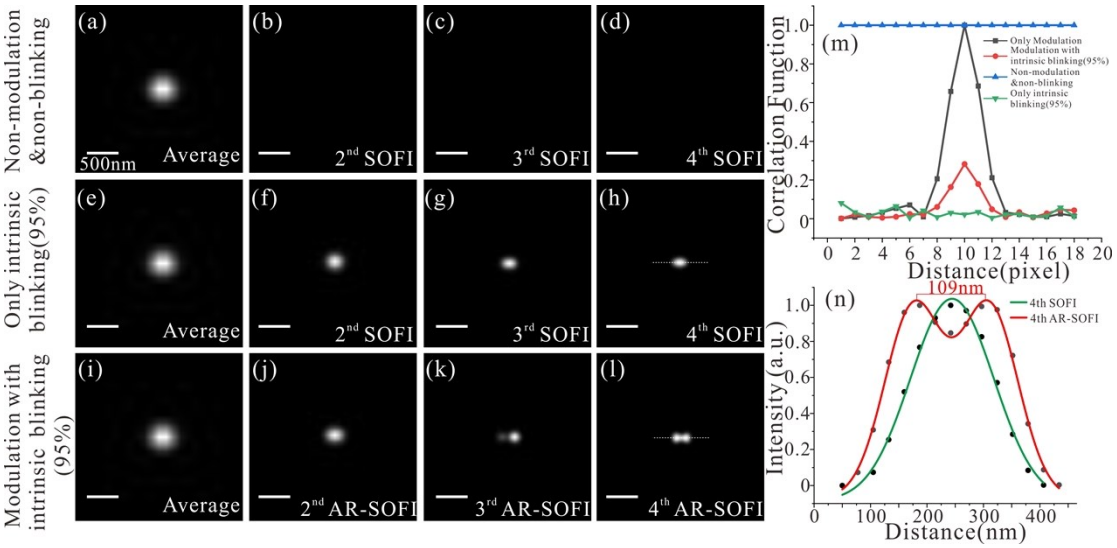

Supplementary Figure S2 The cross-correlation relationships were between adjacent pixels under the combination of active-modulated random illumination (illumination system's PSF: 205 nm) and intrinsic blinking on-time ratio 95% of fluorescent markers. (a) the average image of 1000 wide-field images under non-modulated illumination and non-blinking. (b-c) 2nd, 3rd, and 4th order SOFI reconstruction. (e) the average image of 1000 wide-field images under only intrinsic blinking on-time ratio 95%. (f-h) 2nd, 3rd, and 4th order SOFI reconstruction. (i) the average image of 1000 wide-field images under the combination of active-modulated random illumination and intrinsic blinking on-time ratio 95% of fluorescent markers. (j-l) 2nd, 3rd, and 4th order AR-SOFI reconstruction. (m) the cross-correlation coefficient between adjacent pixels under different conditions, such as only modulation, modulation with intrinsic blinking on-time ratio 95%, non-modulation & non-blinking and only intrinsic blinking on-time ratio 95%. (n) cross-sectional intensity line profiles along the white dashed lines in (h) and (l). Scale bars indicate distances of 500 nm.

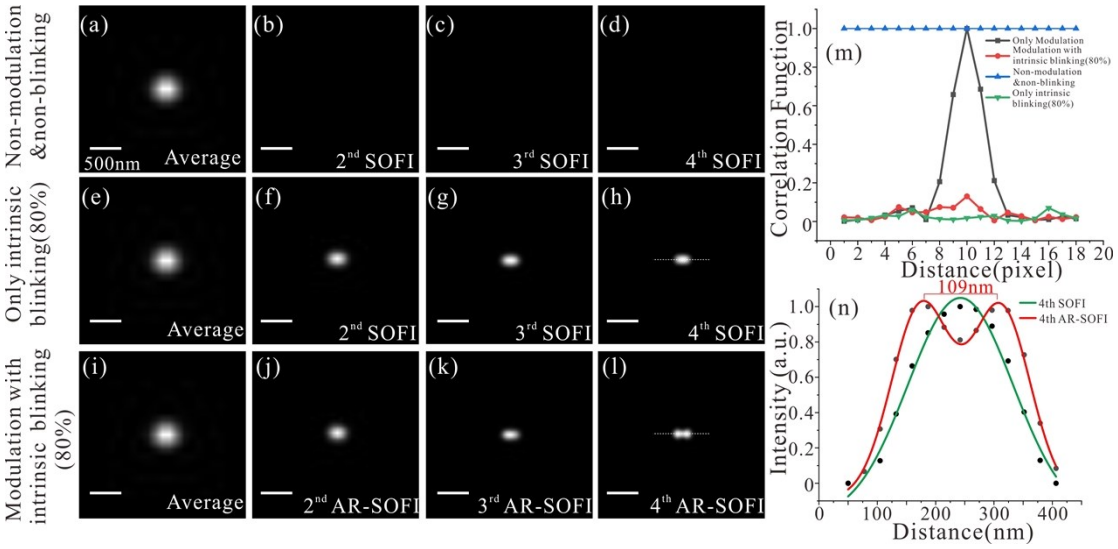

Supplementary Figure S3 The cross-correlation relationships were between adjacent pixels under the combination of active-modulated random illumination (illumination system's PSF: 205 nm) and intrinsic blinking on-time ratio 80% of fluorescent markers. (a) The average image of 1000 wide-field images under non-modulated illumination and non-blinking. (b-c) 2nd, 3rd, and 4th order SOFI reconstruction. (e) the average image of 1000 wide-field images under only intrinsic blinking on-time ratio 80%. (f-h) 2nd, 3rd, and 4th order SOFI reconstruction. (i) The average image of 1000 wide-field images under the combination of active-modulated random illumination and intrinsic blinking on-time ratio 80% of fluorescent markers. (j-l) 2nd, 3rd, and 4th order AR-SOFI reconstruction. (m) The cross-correlation coefficient between adjacent pixels under different conditions, such as only modulation, modulation with intrinsic blinking on-time ratio 80%, non-modulation & non-blinking, and only intrinsic blinking on-time ratio 80%. (n) Cross-sectional intensity line profiles along the white dashed lines in (h) and (l). Scale bars indicate distances of 500 nm.

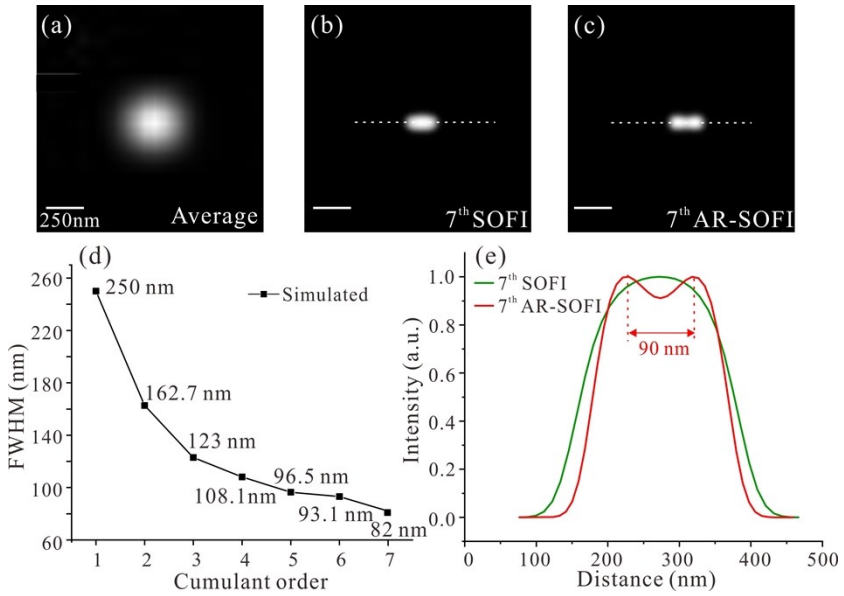

Supplementary Figure S4 The simulated comparison between AR-SOFI and SOFI. (a) the average of 8000 wide-field images with the 90 nm distance of two fluorescent spots. (b) the 7th order SOFI with the 90 nm distance of two fluorescent markers by using 8000 original wide-field images under the impertinent intrinsic on-time ratio (80%). (c) the 7th order AR-SOFI with the 90 nm distance of two fluorescent markers by using 8000 original wide-field images under the combination of active-modulated random illumination and intrinsic blinking on-time ratio 80% of fluorescent markers. (d) full-width-at-half-maximum (FWHM) values of single spot (original FWHM: 250 nm) as a function of cumulant order in simulations. (e) Cross-sectional intensity line profiles along the white dashed lines in (b) and (c).

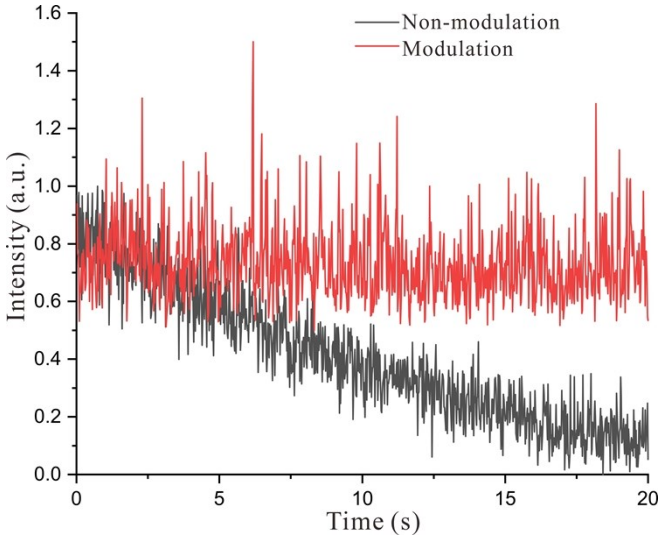

Supplementary Figure S5 Typical fluorescence fluctuations and photostability of Alexa 488 with modulation and non-modulation.

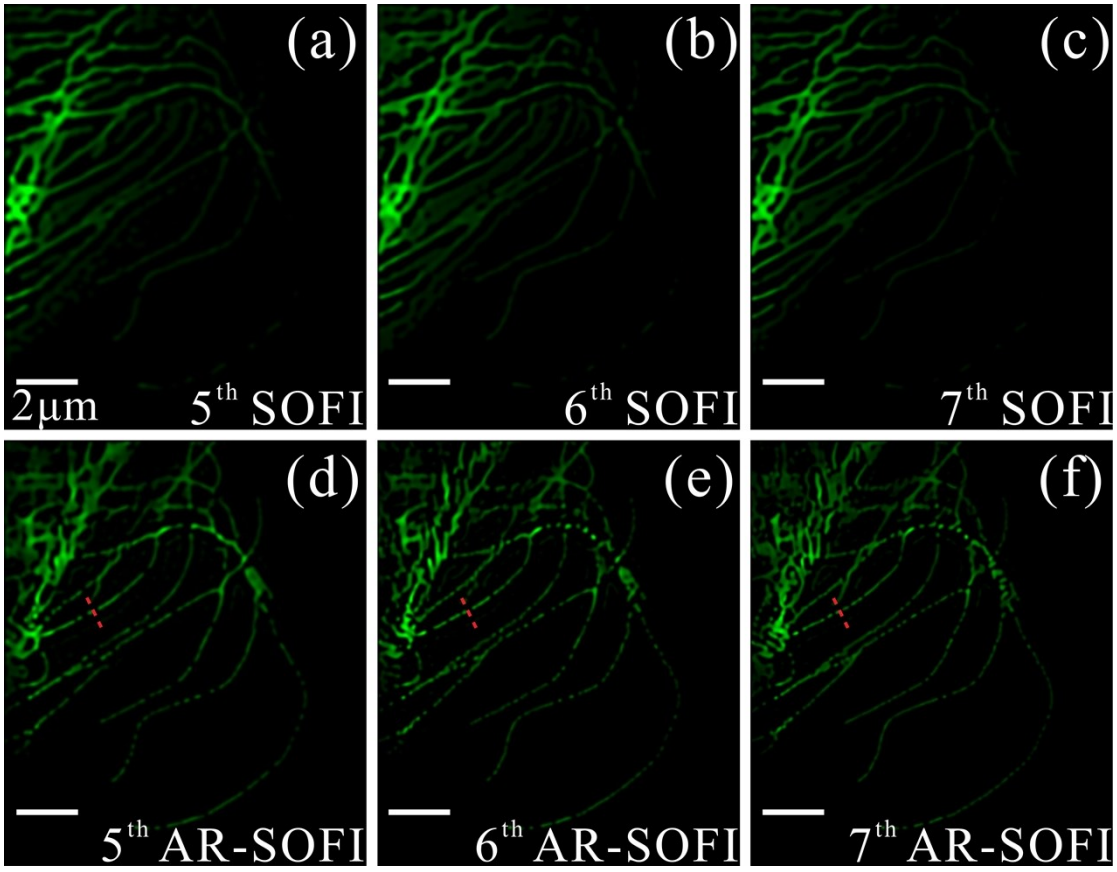

Supplementary Figure S6 Comparison between super-resolution optical fluctuation imaging (SOFI) and active-modulated, random-illumination SOFI (AR-SOFI) processing in microtubules of BS-C-1 labelled with Alexa 488. (a) the 5th order SOFI image. (b) the 6th order SOFI image. (c) the 7th order SOFI image. (d) the 5th order AR-SOFI image. (e) the 6th order AR-SOFI image. (f) the 7th order AR-SOFI image. The scale bars indicate distance of 2 μm.

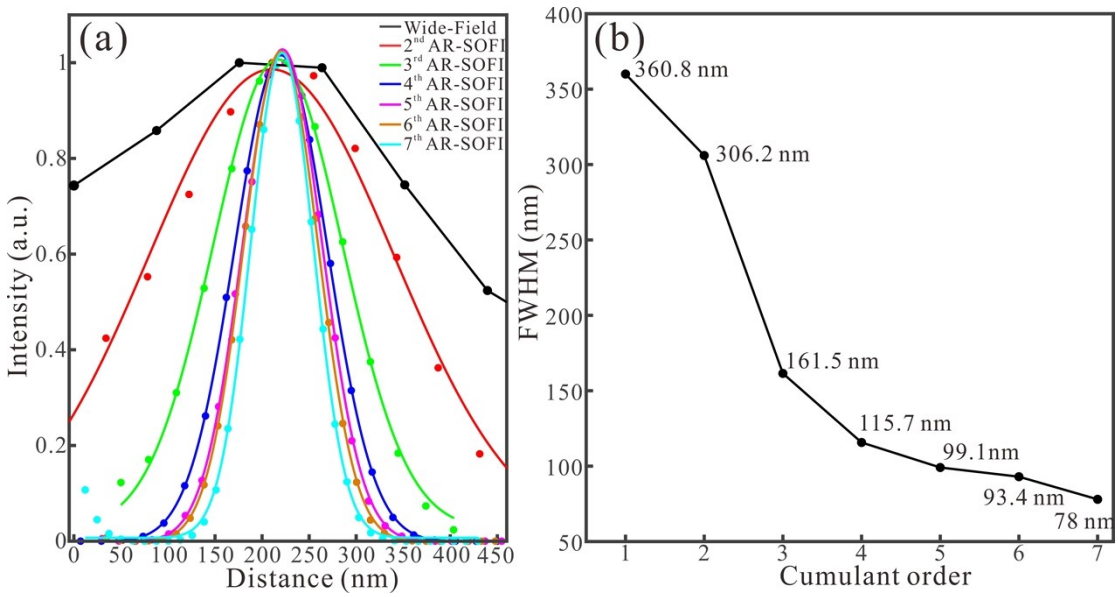

Supplementary Figure S7 Resolution enhancement of different order of AR-SOFI images of the microtubules of BS-C-1 cells labelled with Alexa 488. (a) Intensity profiles along the cross-sections red dotted lines in the Figure 4 and Figure S6. (b) the curves of full-width-half-maximum (FWHM) values versus cumulant order.

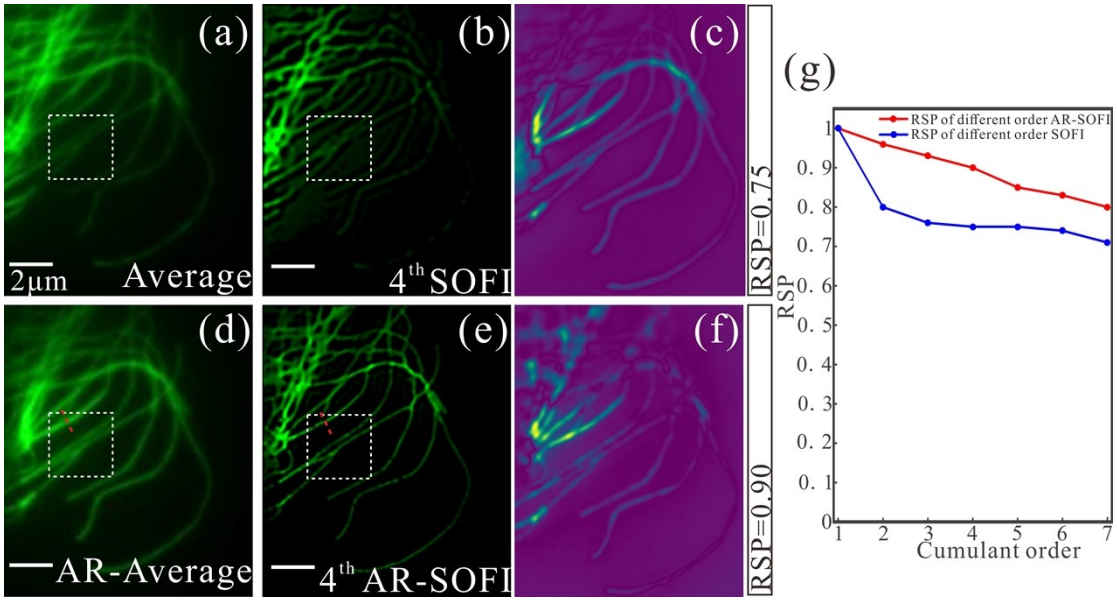

Supplementary Figure S8 Comparison of image qualities between super-resolution optical fluctuation imaging (SOFI) and active-modulated, random-illumination SOFI (AR-SOFI) processing in microtubules of BS-C-1 labelled with Alexa 488. (a) Average image of 1000 wide-field images. (b) the 4th order SOFI image. (c) Error map for 4th order SOFI using the wide-field image in (a) as the reference. (d) Average image from 1000 wide-field images based on active-modulated random illumination. (e) the 4th order AR-SOFI image. (f) Error map for 4th order AR-SOFI using the wide-field image in (d) as the reference. (g) Measurement of RSP value of the different orders reconstructed SOFI or AR-SOFI. The scale bars indicate distance of 2 μm.

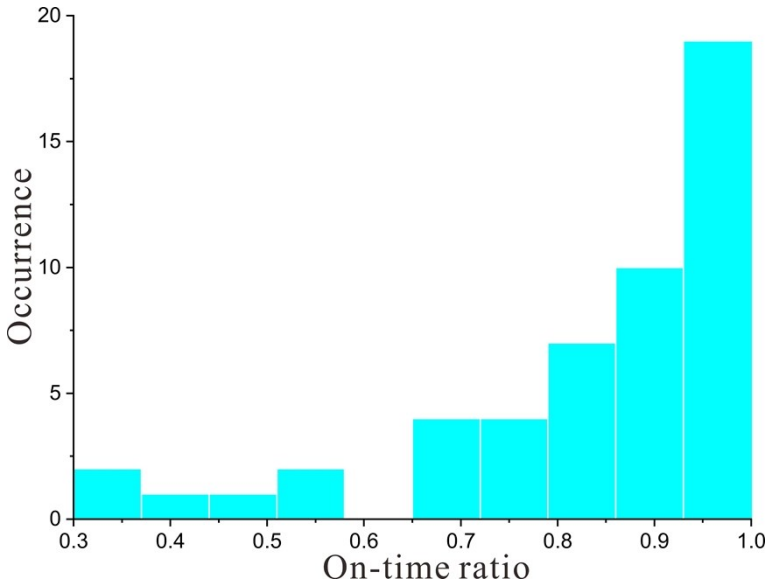

Supplementary Figure S9 Statistical distribution of the on-time ratio based on single-particle statistics for quantum dot (n=50)

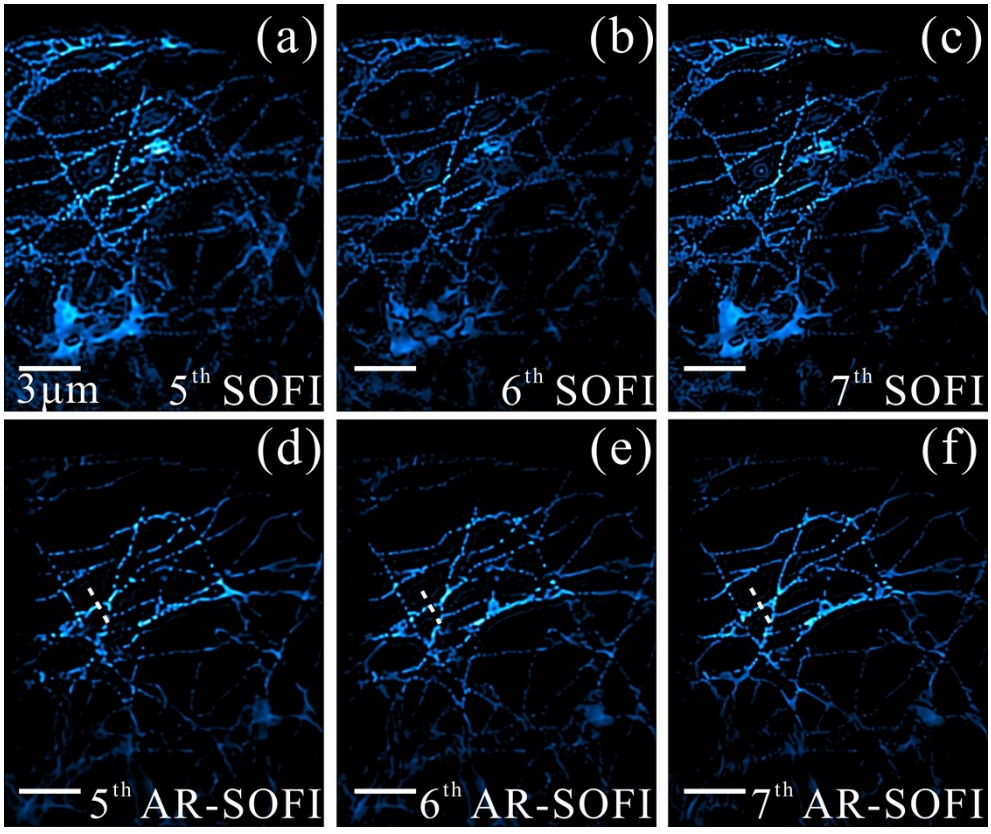

Supplementary Figure S10 Comparison between SOFI and AR-SOFI processing in microtubules of BS-C-1 cells labelled with QDs655. (a) 5th order SOFI image. (b) the 6th order SOFI image. (c) the 7th order SOFI image. (d) the 5th order AR-SOFI image. (e) the 6th order AR-SOFI image. (f) the 7th order AR-SOFI image. The scale bars indicate distance of 3 μm

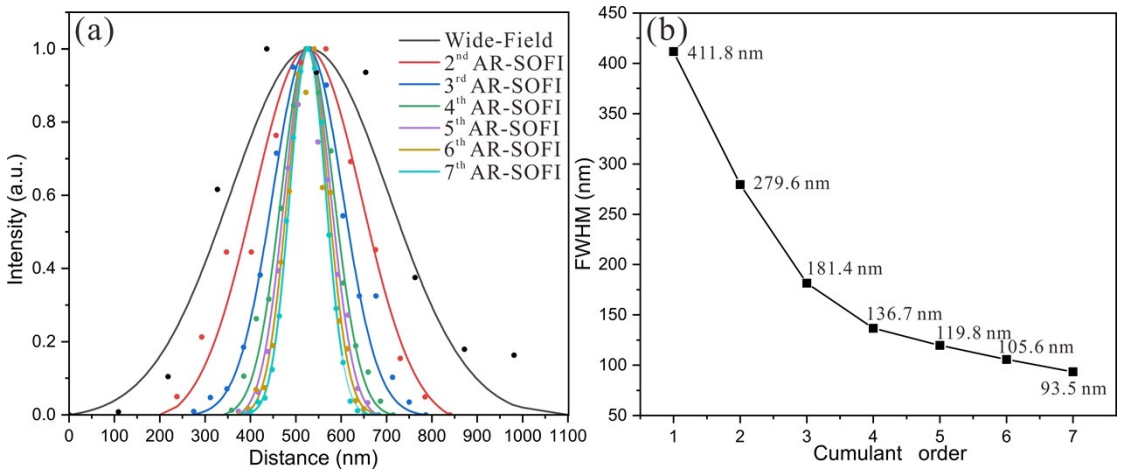

Supplementary Figure S11 Resolution enhancement of different order of AR-SOFI images in microtubules of BS-C-1 cells labelled with QDs655. (a) Intensity profiles along the cross-sections white dotted lines in the Figure 5 and Figure S10. (b) the curves of FWHM values versus cumulant order.

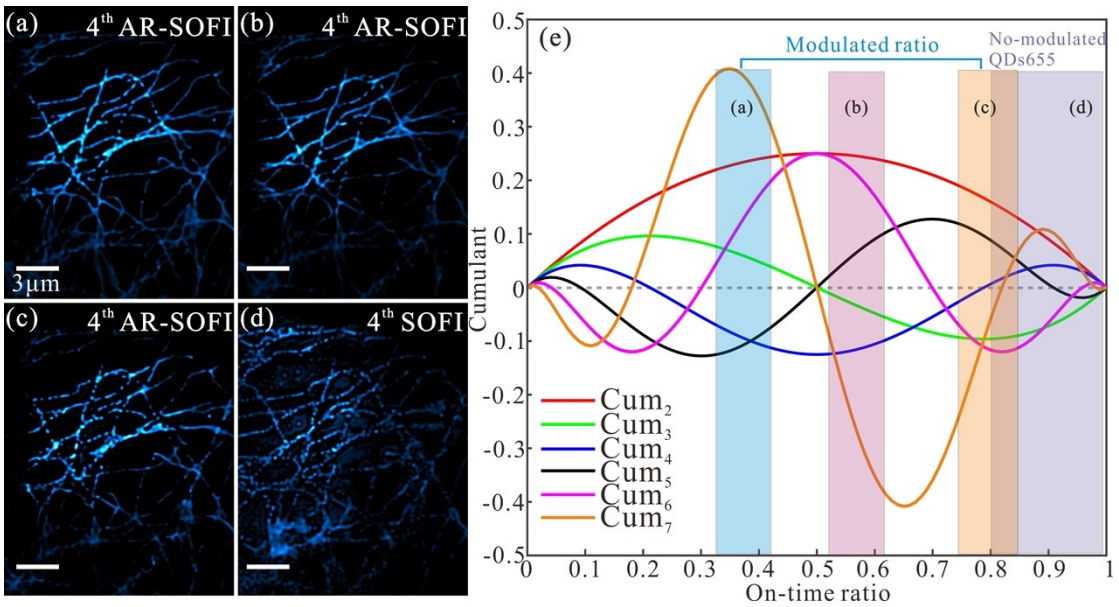

Supplementary Figure S12 4th order AR-SOFI and SOFI images in the microtubules of BS-C-1 cells labeled with QDs655 under controllable different on-time ratio. (a) 4th order AR-SOFI for on-time ratio in the range of 34% and 43%. (b) 4th order AR-SOFI for on-time ratio in the range of 53% and 62%. (c) 4th order AR-SOFI for on-time ratio in the range of 75% and 84%. (d) 4th order SOFI for on-time ratio in the range of 80% and 100%. (e) the schematic diagram of different on-time ratio distribution based on the SLM, corresponding to (a-d), respectively.

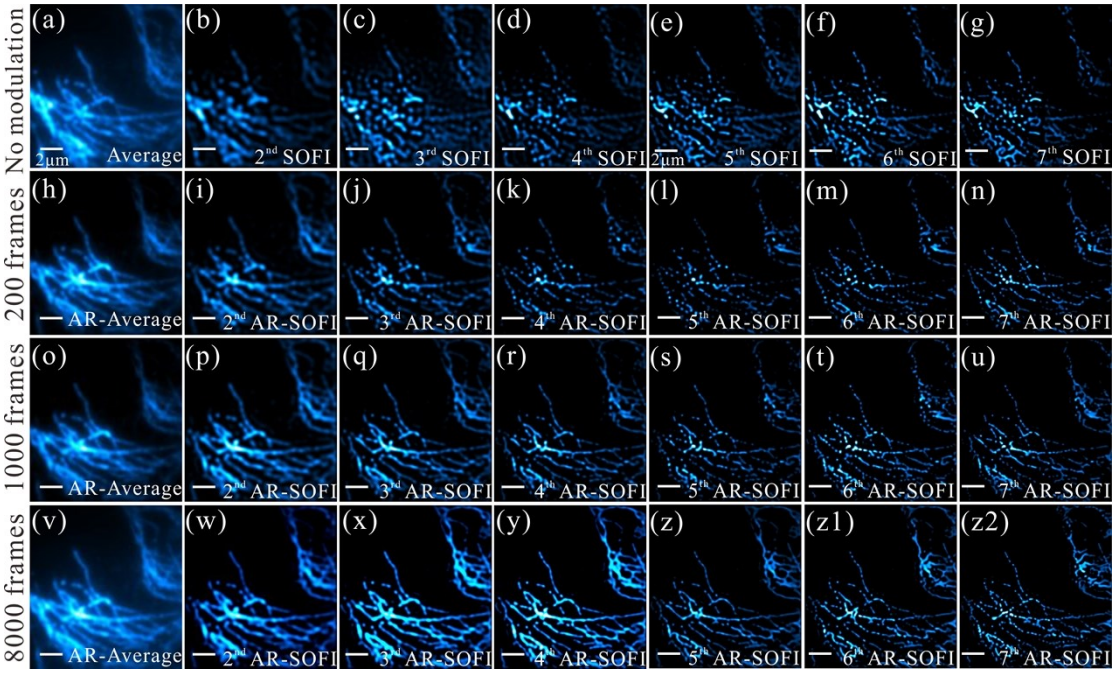

Supplementary Figure S13 Comparison between SOFI and AR-SOFI processing in microtubules of BS-C-1 cells labelled with QDs655 using 8000-frame wide-field images. (a) Average image of 8000-frame non-modulated wide-field images. (b-g) 2nd-7th order SOFI reconstruction by using 8000-frame non-modulated wide-field images. (h) Average image of 200-frame wide-field images by active-modulated random illumination. (i-n) 2nd-7th order AR-SOFI reconstruction by using 200-frame modulated wide-field images. (o) Average image of 1000-frame modulated wide-field images. (p-u) 2nd-7th order AR-SOFI reconstruction by using 1000-frame modulated wide-field images. (v) Average image of 8000-frame modulated wide-field images. (w-z2) 2nd-7th order AR-SOFI reconstruction by using 8000-frame modulated wide-field images. The scale bars indicate distance of 2 μm.

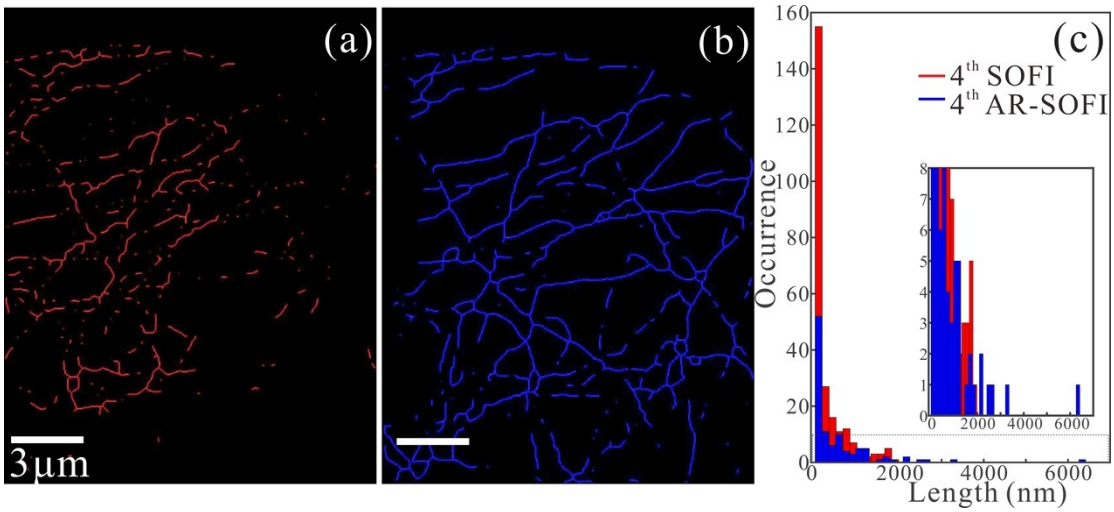

Supplementary Figure S14 Comparison of the continuities of 4th order SOFI and 4th order AR-SOFI. (a), (b) Skeletonized images of Figure 5(d) and Figure 5(h), in which the long continuous microtubules are predominant in Figure 5(h). (c) Histograms of the length of the continuous line in (a) and (b) are plotted. Scale bars: 3 μm.

Supplementary References

1. S. Geissbuehler, N. L. Bocchio, C. Dellagiacoma, C. Berclaz, M. Leutenegger and T. Lasser, *Optical Nanoscopy*, 2012, **1**, 4.
2. X. Yi and S. Weiss, *Biomedical Optics Express*, 2020, **11**, 554-570.
3. Z. Sun, Z. Liu, H. Chen, R. Li, Y. Sun, D. Chen, G. Xu, L. Liu and C. Wu, *Advanced Optical Materials*, 2019, **7**, 1900007.
4. T.-C. Lee, R. L. Kashyap and C.-N. Chu, *CVGIP: Graphical Models and Image Processing*, 1994, **56**, 462-478.
5. R. F.-G. Ignacio Arganda-Carreras, Arrate Munoz-Barrutia, Carlos Ortiz-De-Solorzano, *Microscopy Research & Technique*, 2010, **73**, 1019-1029.